Dynamic Scene Deblurring Using Spatially Variant Recurrent Neural Networks Supplemental Material

Anonymous CVPR submission

Paper ID 1193

Overview

In this supplemental material, we first analyze the effect of the proposed spatially variant RNN on image deblurring in Section 1. Then we quantitatively evaluate our method on the publicly available datasets (including the dynamic scene deblurring dataset [6] and real-world video deblurring datasets by Cho et al. [1] and Su et al. [9]) in Sections 2, 3 and 4, respectively.

1. Effect of the proposed spatially variant RNN

We note that conventional dynamic scene deblurring algorithms [7, 3] usually use segmentation methods to segment the objects with different motion blurs, and then apply the deblurring algorithms to the segmented objects. Specifically, the segmentation results are actually regarded as the confidence map (i.e., weights in [7, 3]) in the deblurring models, so that each segmented regions has its own deblurring model. Our algorithm has the similar effect to these conventional algorithms. Our CNNs first extract the features and then they are used to guide the weight of the spatial variant RNN for image deblurring. Figure 1 shows that extracted the features are able to distinguish the moving objects, e.g., the moving car (Figure 1(e)). Thus, under the guidance of the extracted the features, the proposed algorithm is able to recover a clear image as shown in Figure 1(c).

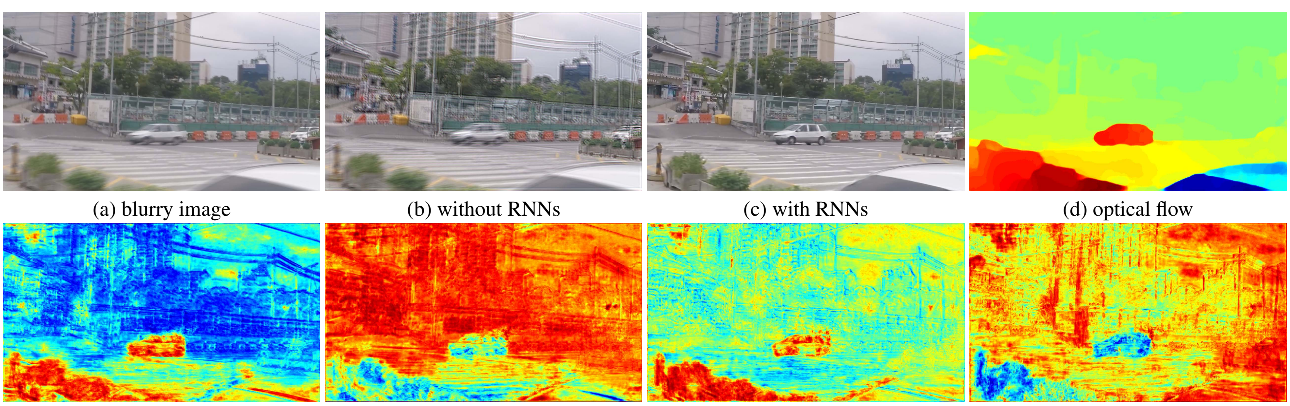

(a) blurry image (b) without RNNs (c) with RNNs (d) optical flow

(e) RNN weights

Figure 1. Effect of the proposed spatially variant RNN. (a) is the blurry image. (b) and (c) are the output of the network without and with RNNs respectively. (d) is the optical flow from the adjacent frames of (a) according to FlowNet 2.0 [4] and (e) are four selected RNN weights from the proposed network. The RNN weights are consistent with the object motions and can remove the blur from (b).

2. Comparisons on the dynamic scene deblurring dataset [6]

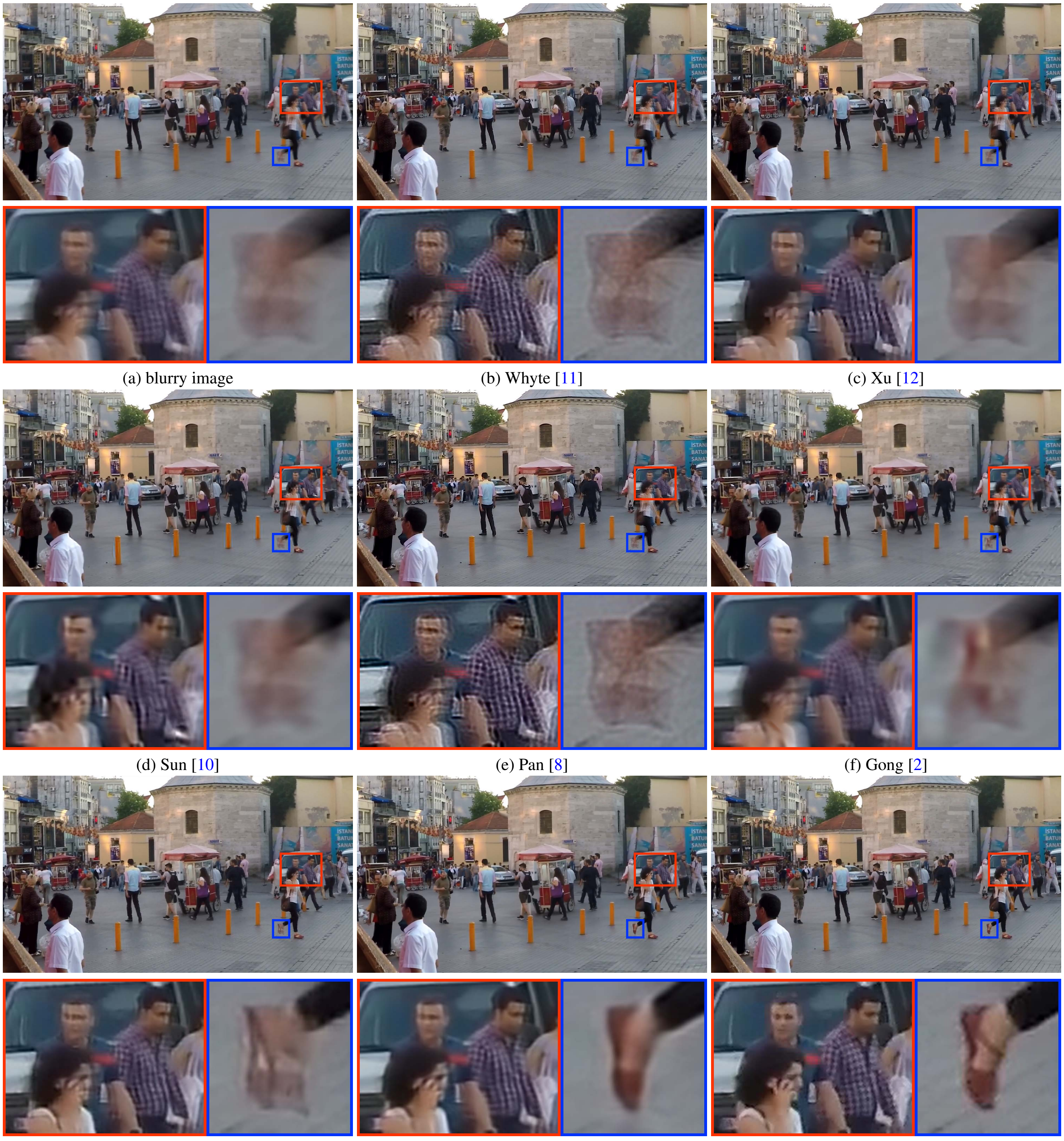

(a) blurry image (b) Whyte [11] (c) Xu [12]
(d) Sun [10] (e) Pan [8] (f) Gong [2]
(g) Nah [6] (h) the proposed method (i) clean image

Figure 2. Visual comparison for the dynamic scene deblurring dataset [6].

(a) blurry image (b) Whyte [11] (c) Xu [12]

(d) Sun [10] (e) Pan [8] (f) Gong [2]

(g) Nah [6] (h) the proposed method (i) clean image

Figure 3. Visual comparison for the dynamic scene deblurring dataset [6].

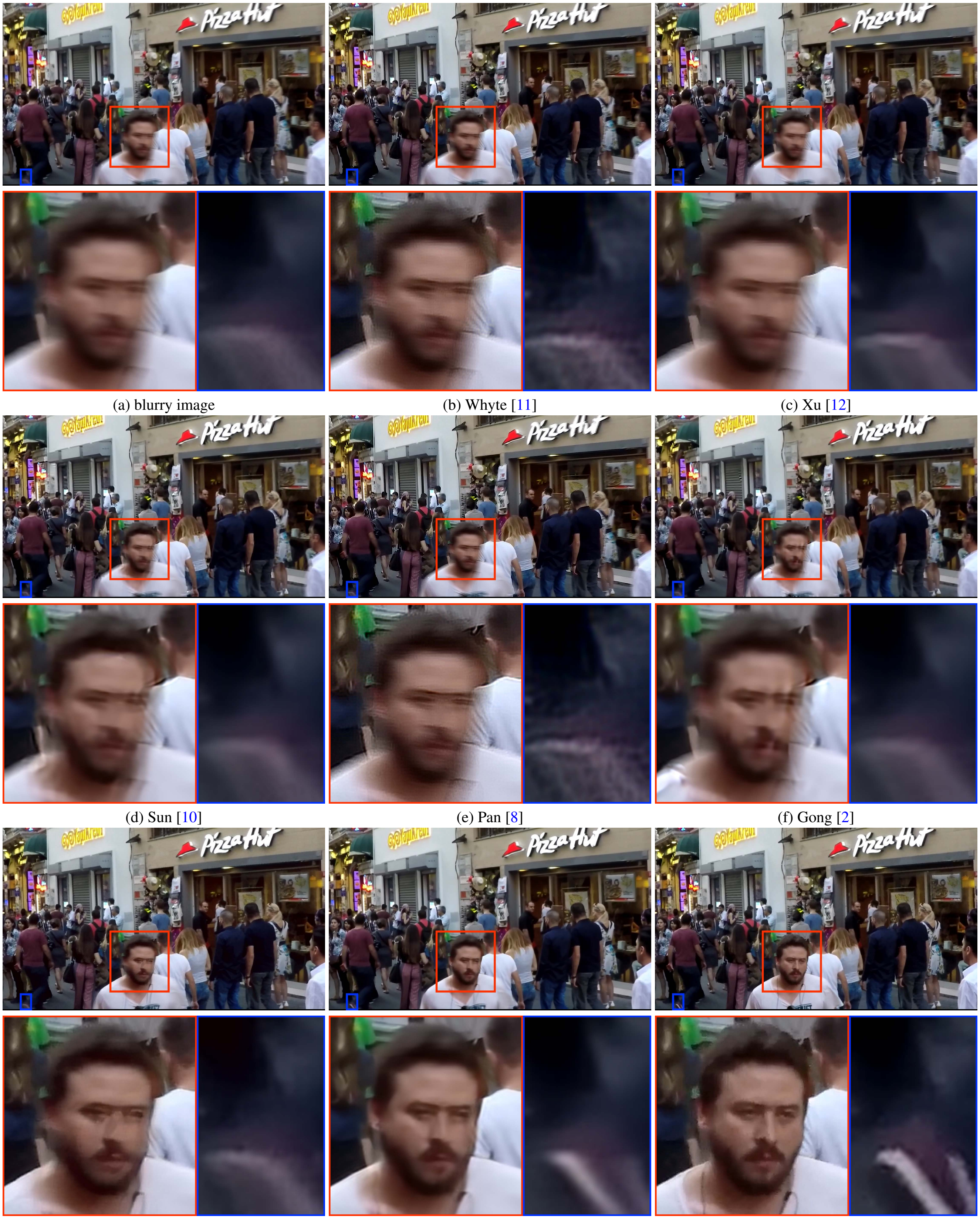

(a) blurry image (b) Whyte [11] (c) Xu [12]

(d) Sun [10] (e) Pan [8] (f) Gong [2]

(g) Nah [6] (h) the proposed method (i) clean image

Figure 4. Visual comparison for the dynamic scene deblurring dataset [6].

CVPR #1193

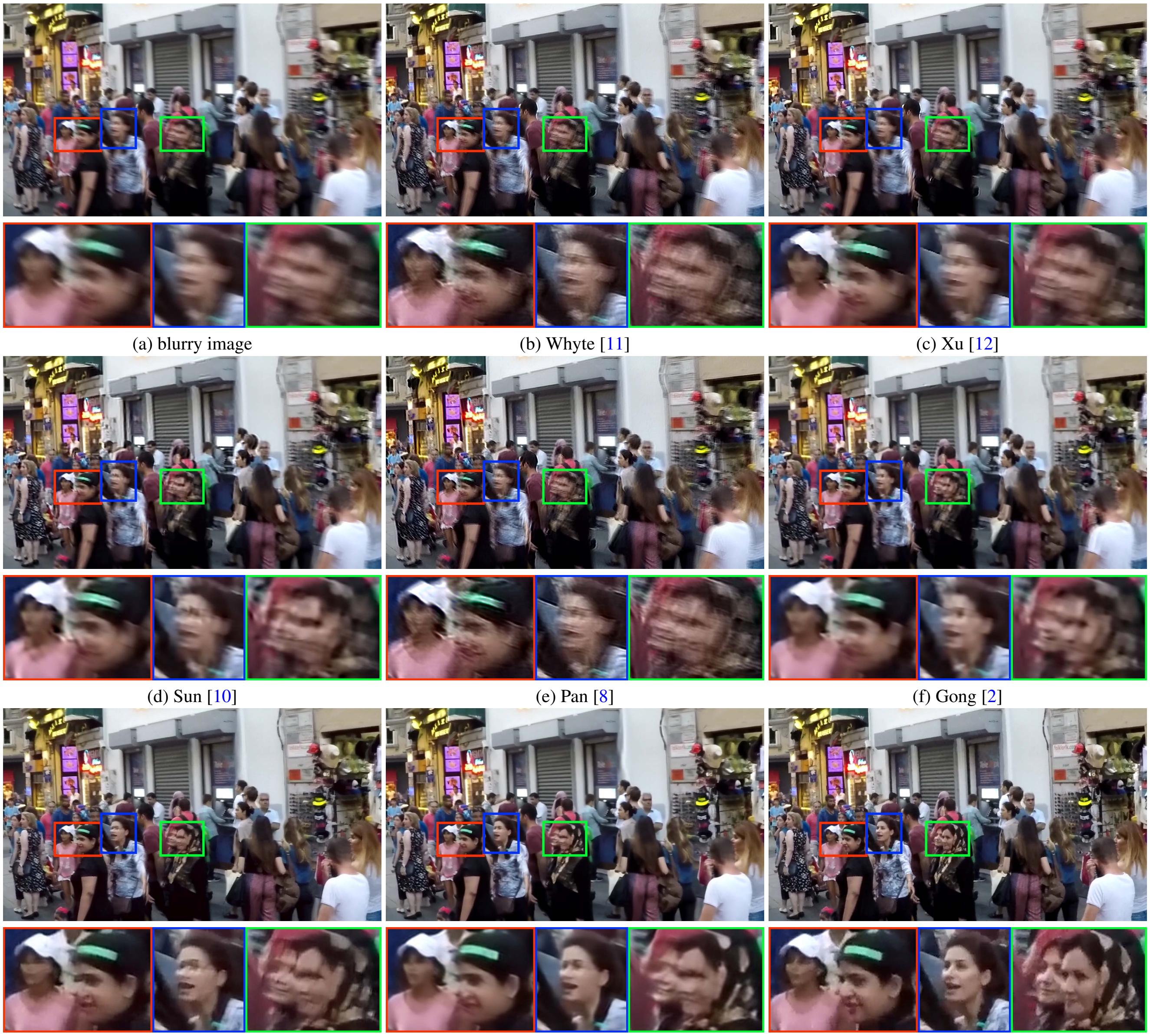

(a) blurry image (b) Whyte [11] (c) Xu [12]

(d) Sun [10] (e) Pan [8] (f) Gong [2]

(g) Nah [6] (h) the proposed method (i) clean image

Figure 5. Visual comparison for the dynamic scene deblurring dataset [6].

CVPR #1193

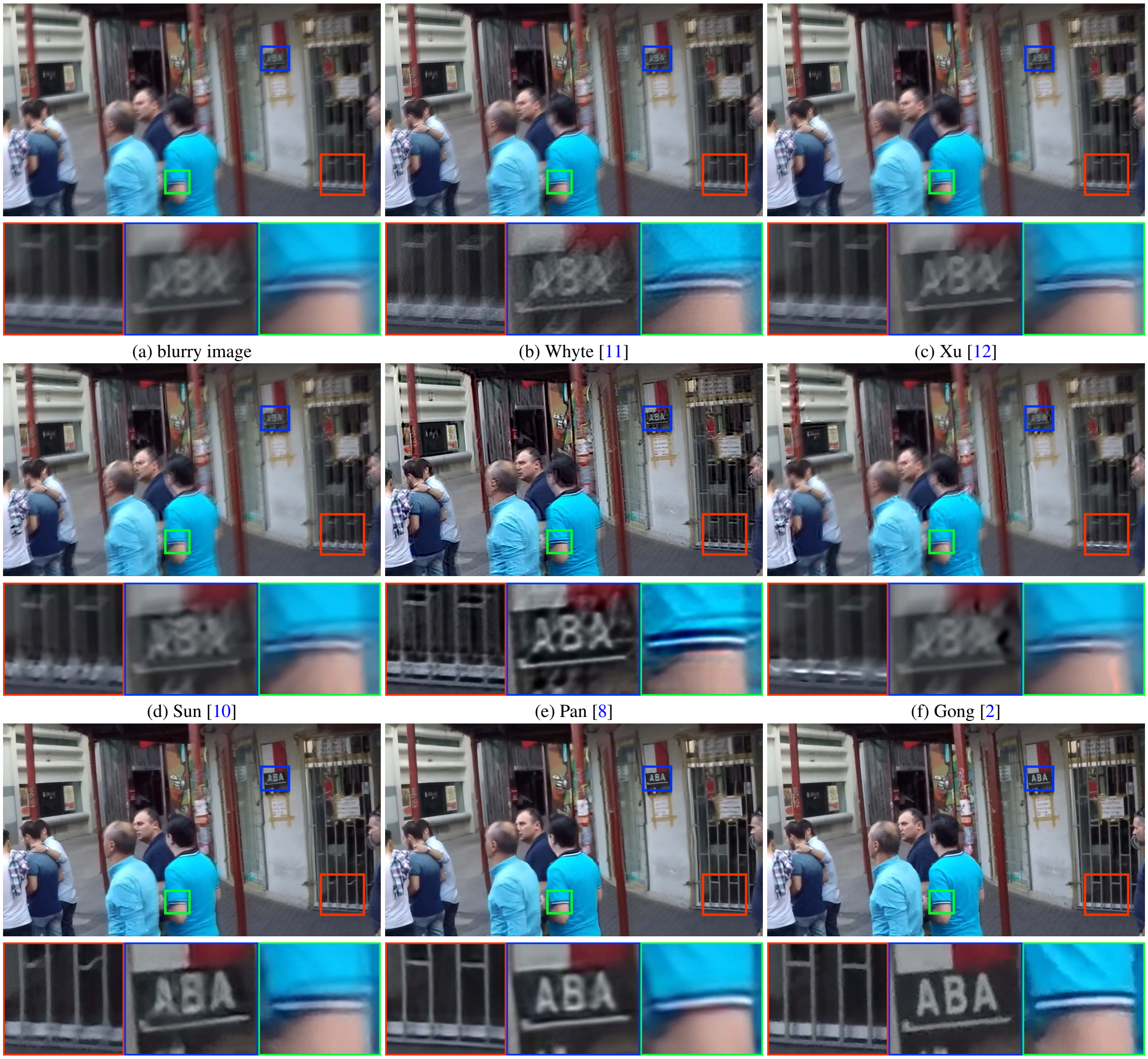

(a) blurry image (b) Whyte [11] (c) Xu [12]

(d) Sun [10] (e) Pan [8] (f) Gong [2]

(g) Nah [6] (h) the proposed method (i) clean image

Figure 6. Visual comparison for the dynamic scene deblurring dataset [6].

(a) blurry image (b) Whyte [11] (c) Xu [12]

(d) Sun [10] (e) Pan [8] (f) Gong [2]

(g) Nah [6] (h) the proposed method (i) clean image

Figure 7. Visual comparison for the dynamic scene deblurring dataset [6].

(a) blurry image (b) Whyte [11] (c) Xu [12]
(d) Sun [10] (e) Pan [8] (f) Gong [2]
(g) Nah [6] (h) the proposed method (i) clean image

Figure 8. Visual comparison for the dynamic scene deblurring dataset [6].

CVPR #1193

(a) blurry image (b) Whyte [11] (c) Xu [12]

(d) Sun [10] (e) Pan [8] (f) Gong [2]

(g) Nah [6] (h) the proposed method (i) clean image

Figure 9. Visual comparison for the dynamic scene deblurring dataset [6].

(a) blurry image (b) Whyte [11] (c) Xu [12]

(d) Sun [10] (e) Pan [8] (f) Gong [2]

(g) Nah [6] (h) the proposed method (i) clean image

Figure 10. Visual comparison for the dynamic scene deblurring dataset [6].

(a) blurry image (b) Whyte [11] (c) Xu [12]

(d) Sun [10] (e) Pan [8] (f) Gong [2]

(g) Nah [6] (h) the proposed method (i) clean image

Figure 11. Visual comparison for the dynamic scene deblurring dataset [6].

CVPR #1193

(a) blurry image (b) Whyte [11] (c) Xu [12]

(d) Sun [10] (e) Pan [8] (f) Gong [2]

(g) Nah [6] (h) the proposed method (i) clean image

Figure 12. Visual comparison for the dynamic scene deblurring dataset [6].

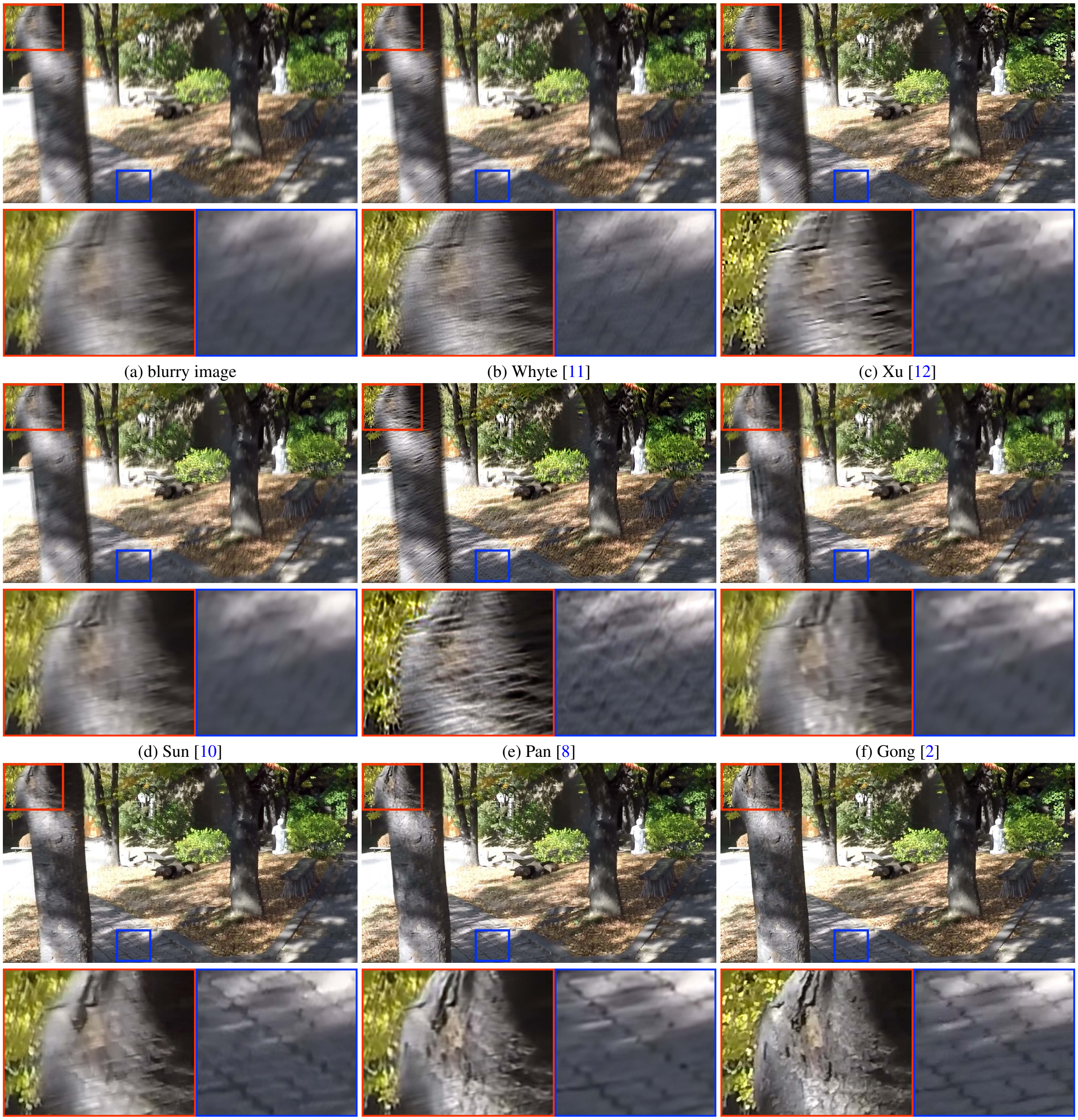

(a) blurry image (b) Whyte [11] (c) Xu [12]
(d) Sun [10] (e) Pan [8] (f) Gong [2]
(g) Nah [6] (h) the proposed method (i) clean image

Figure 13. Visual comparison for the dynamic scene deblurring dataset [6].

(a) blurry image (b) Whyte [11] (c) Xu [12]

(d) Sun [10] (e) Pan [8] (f) Gong [2]

(g) Nah [6] (h) the proposed method (i) clean image

Figure 14. Visual comparison for the dynamic scene deblurring dataset [6].

CVPR #1193

(a) blurry image (b) Whyte [11] (c) Xu [12]
(d) Sun [10] (e) Pan [8] (f) Gong [2]
(g) Nah [6] (h) the proposed method (i) clean image

Figure 15. Visual comparison for the dynamic scene deblurring dataset [6].

(a) blurry image (b) Whyte [11] (c) Xu [12]
(d) Sun [10] (e) Pan [8] (f) Gong [2]
(g) Nah [6] (h) the proposed method (i) clean image

Figure 16. Visual comparison for the dynamic scene deblurring dataset [6].

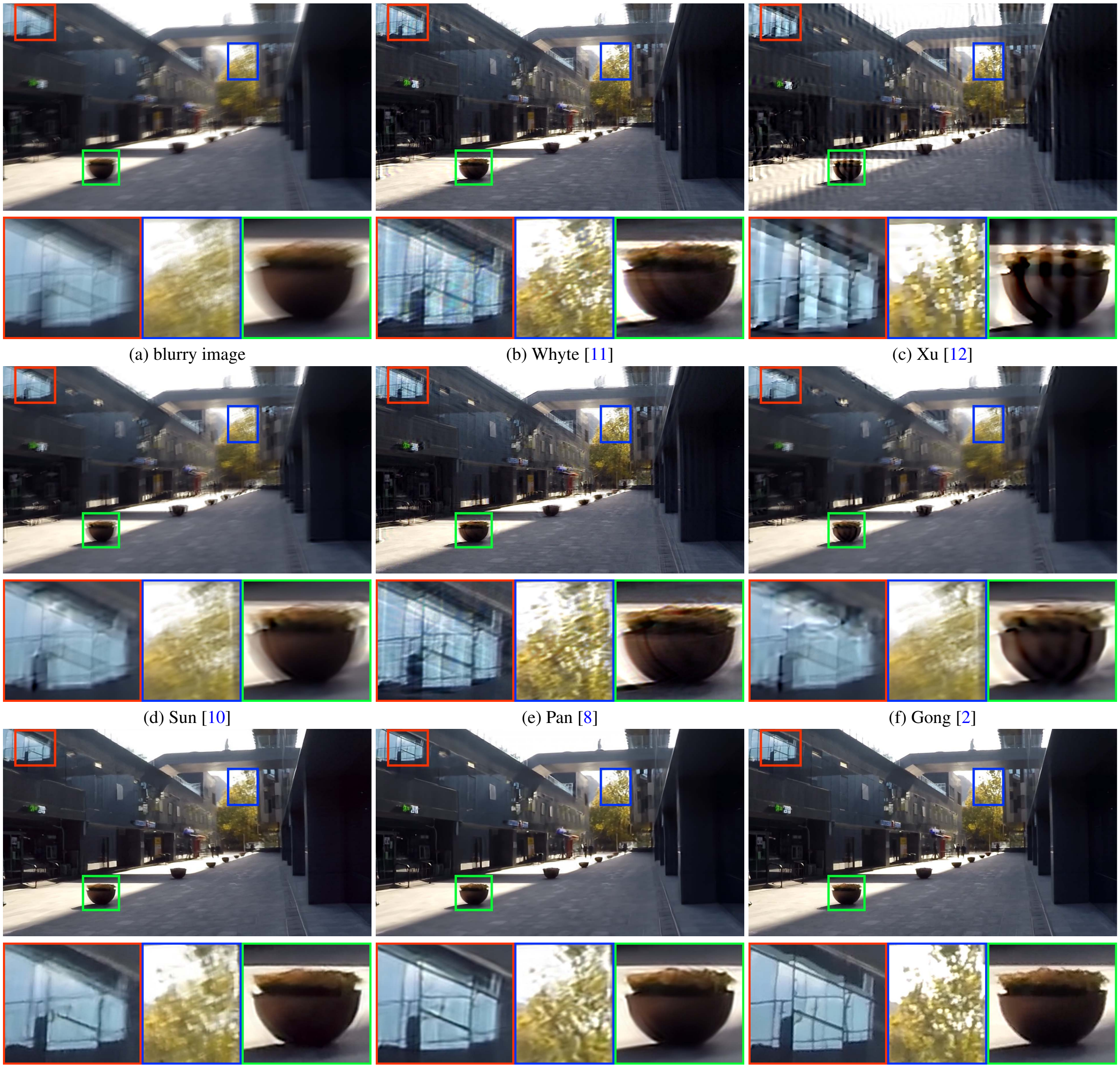

(a) blurry image (b) Whyte [11] (c) Xu [12]
(d) Sun [10] (e) Pan [8] (f) Gong [2]
(g) Nah [6] (h) the proposed method (i) clean image

Figure 17. Visual comparison for the dynamic scene deblurring dataset [6].

3. Comparisons on the real-world blurred video dataset [1]

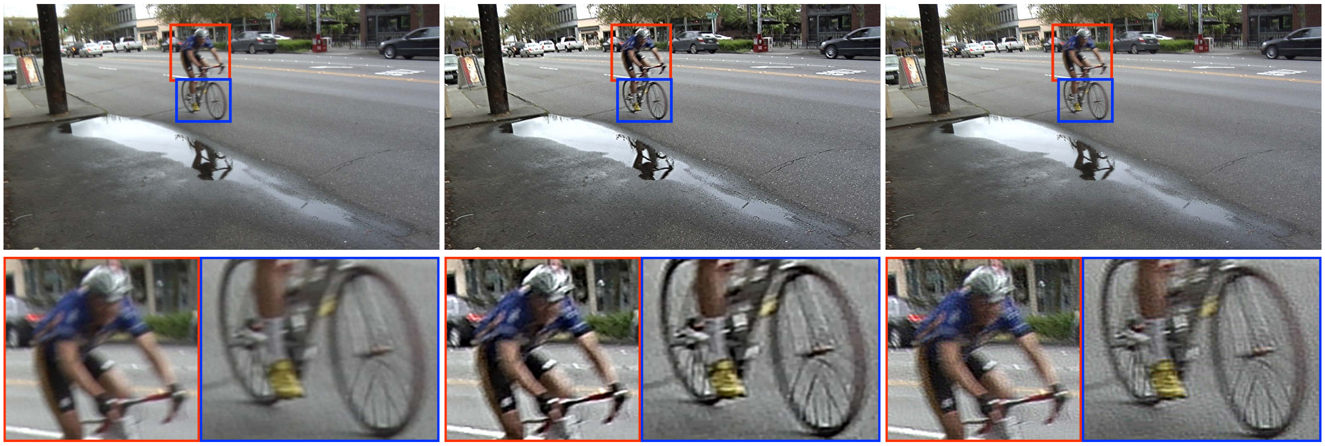

(a) blurry image (b) Krishnan [5] (c) Whyte [11]

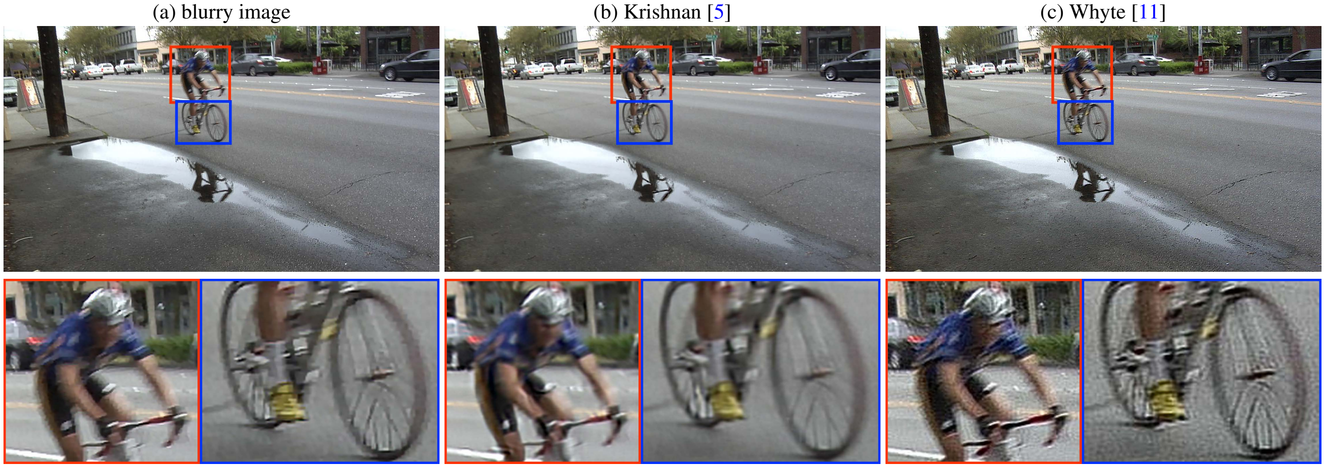

(d) Xu [12] (e) Sun [10] (f) Pan [8]

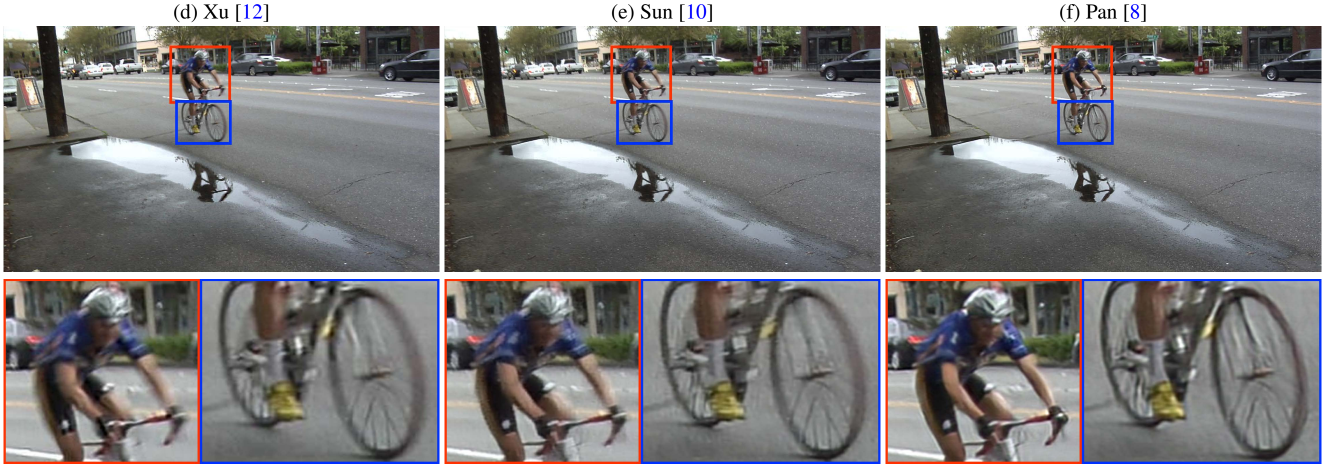

(g) Gong [2] (h) Nah [6] (i) the proposed method

Figure 18. Visual comparison for the real blurry image dataset [1].

(a) blurry image (b) Krishnan [5] (c) Whyte [11]
(d) Xu [12] (e) Sun [10] (f) Pan [8]
(g) Gong [2] (h) Nah [6] (i) the proposed method

Figure 19. Visual comparison for the real blurry image dataset [1].

(a) blurry image (b) Krishnan [5] (c) Whyte [11]

(d) Xu [12] (e) Sun [10] (f) Pan [8]

(g) Gong [2] (h) Nah [6] (i) the proposed method

Figure 20. Visual comparison for the real blurry image dataset [1].

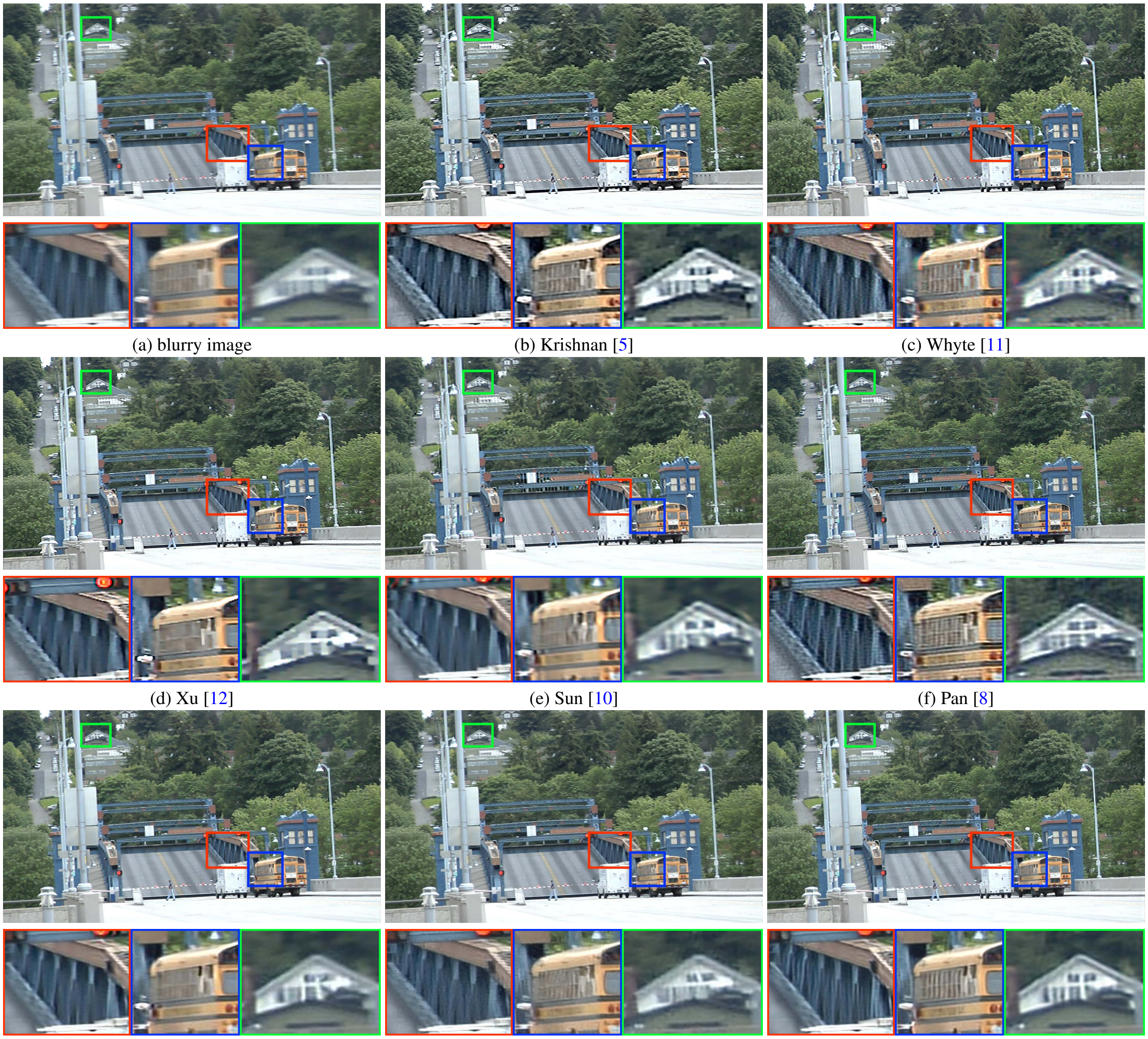

(a) blurry image (b) Krishnan [5] (c) Whyte [11]
(d) Xu [12] (e) Sun [10] (f) Pan [8]
(g) Gong [2] (h) Nah [6] (i) the proposed method

Figure 21. Visual comparison for the real blurry image dataset [1].

CVPR
#1193

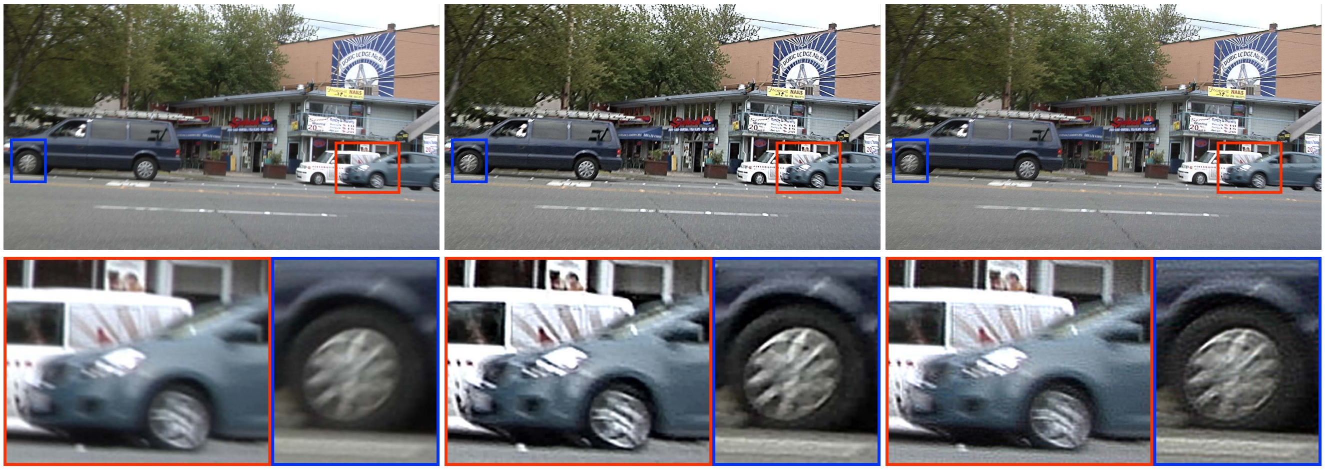

(a) blurry image (b) Krishnan [5] (c) Whyte [11]

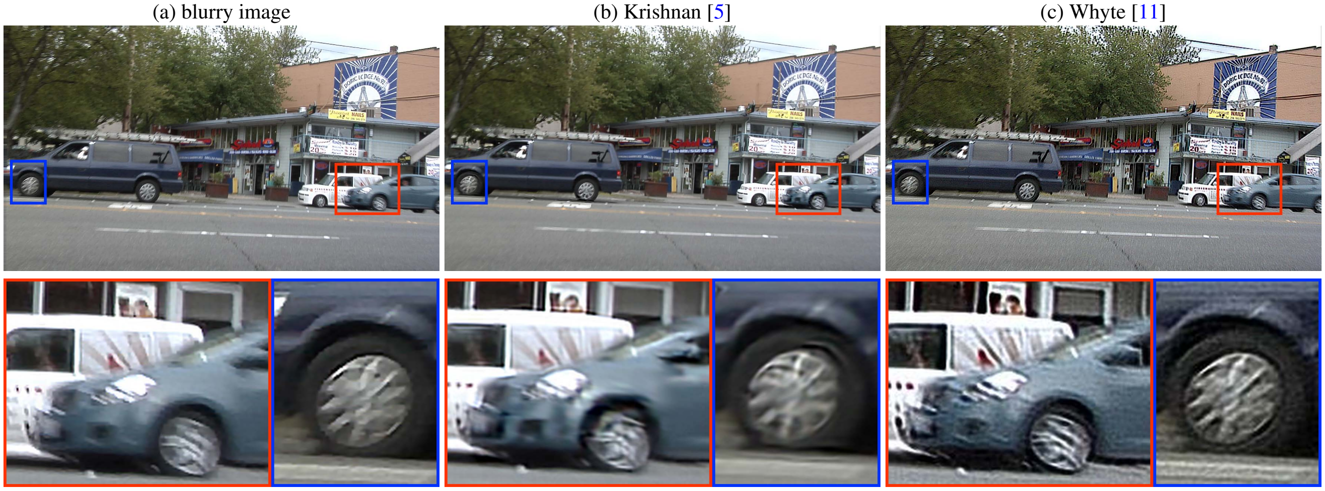

(d) Xu [12] (e) Sun [10] (f) Pan [8]

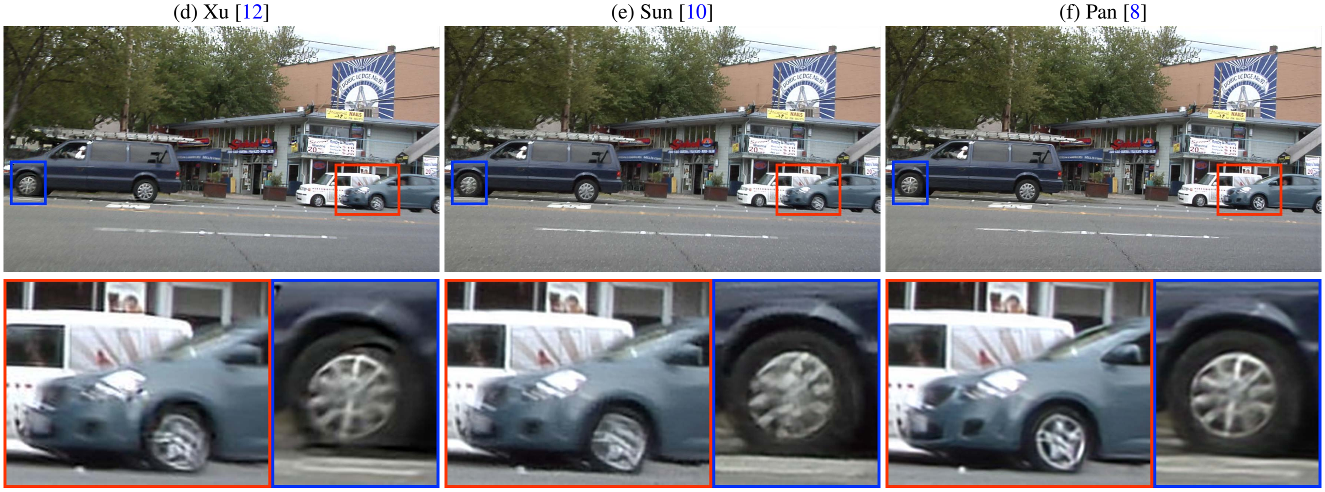

(g) Gong [2] (h) Nah [6] (i) the proposed method

Figure 22. Visual comparison for the real blurry image dataset [1].

4. Comparisons on the video deblurring dataset [9]

(a) blurry image (b) Krishnan [5] (c) Whyte [11]

(d) Xu [12] (e) Sun [10] (f) Pan [8]

(g) Gong [2] (h) Nah [6] (i) the proposed method

Figure 23. Visual comparison for the video deblurring dataset [9].

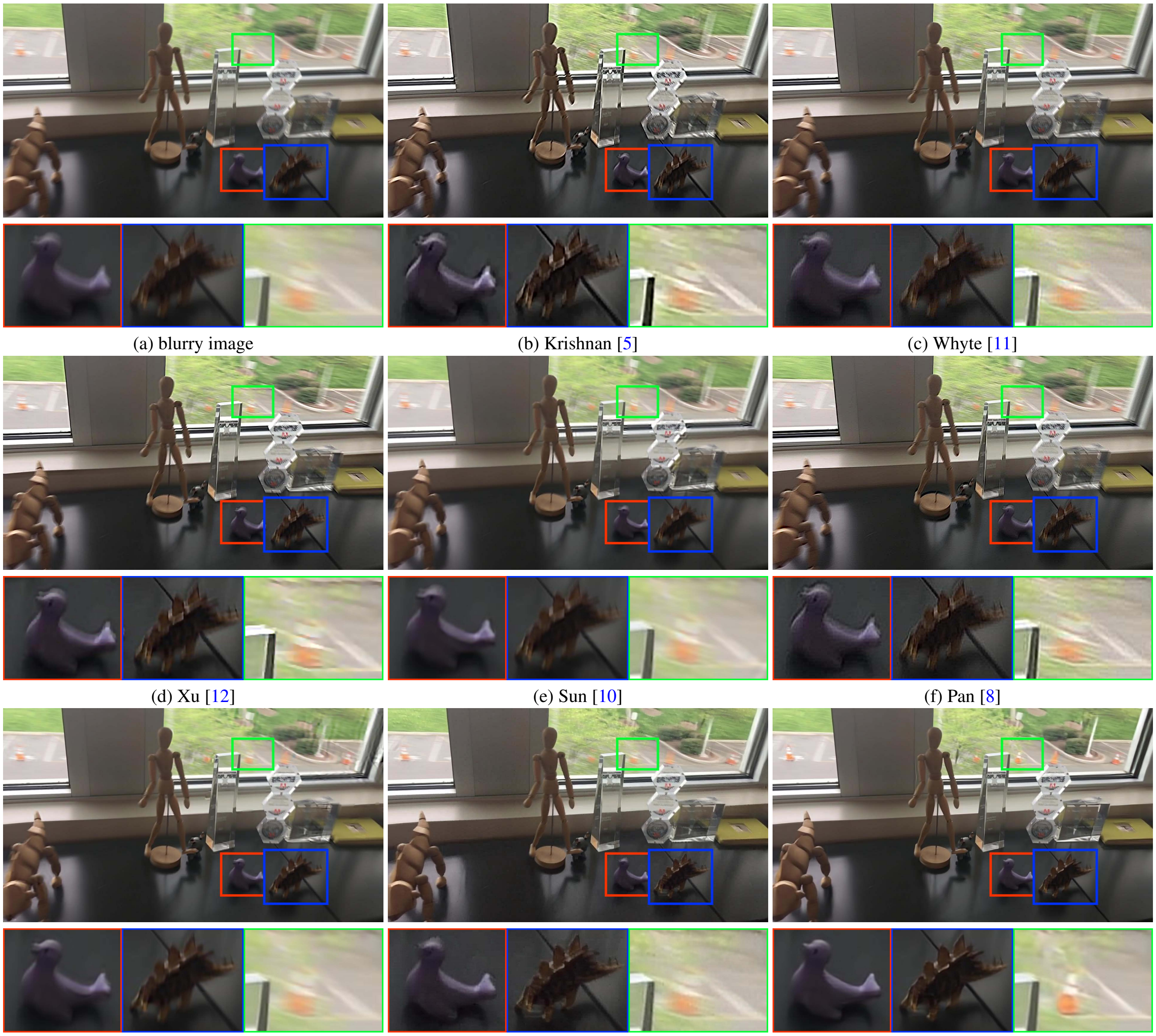

(a) blurry image (b) Krishnan [5] (c) Whyte [11]

(d) Xu [12] (e) Sun [10] (f) Pan [8]

(g) Gong [2] (h) Nah [6] (i) the proposed method

Figure 24. Visual comparison for the video deblurring dataset [9].

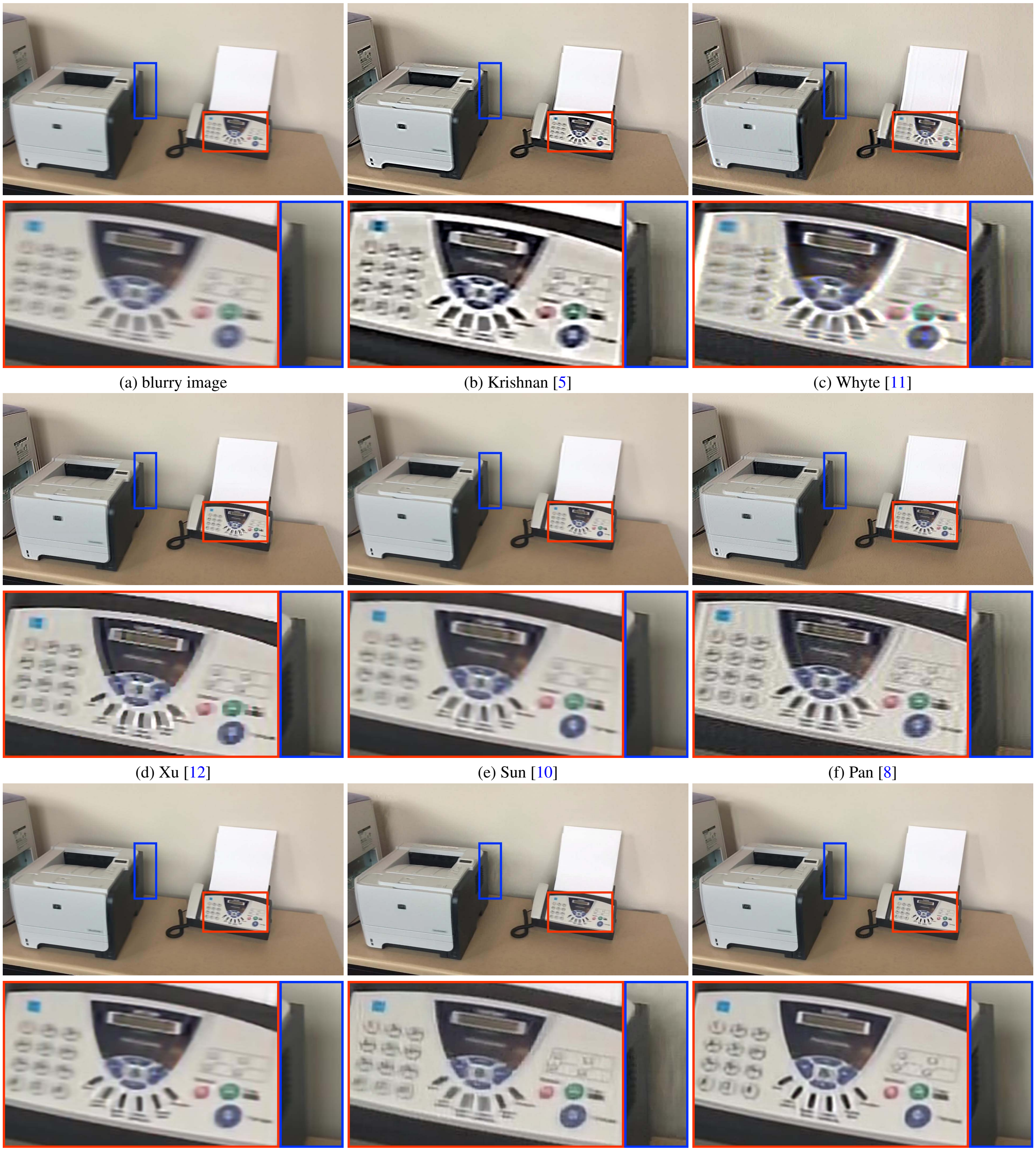

(a) blurry image (b) Krishnan [5] (c) Whyte [11]
(d) Xu [12] (e) Sun [10] (f) Pan [8]
(g) Gong [2] (h) Nah [6] (i) the proposed method

Figure 25. Visual comparison for the video deblurring dataset [9].

(a) blurry image (b) Krishnan [5] (c) Whyte [11]

(d) Xu [12] (e) Sun [10] (f) Pan [8]

(g) Gong [2] (h) Nah [6] (i) the proposed method

Figure 26. Visual comparison for the video deblurring dataset [9].

References

[1] S. Cho, J. Wang, and S. Lee. Video deblurring for hand-held cameras using patch-based synthesis. *TOG*, 2012. 1, 18, 19, 20, 21, 22

[2] D. Gong, J. Yang, L. Liu, Y. Zhang, I. Reid, C. Shen, A. v. d. Hengel, and Q. Shi. From motion blur to motion flow: a deep learning solution for removing heterogeneous motion blur. In *CVPR*, 2017. 2, 3, 4, 5, 6, 7, 8, 9, 10, 11, 12, 13, 14, 15, 16, 17, 18, 19, 20, 21, 22, 23, 24, 25, 26

[3] T. Hyun Kim, B. Ahn, and K. Mu Lee. Dynamic scene deblurring. In *ICCV*, 2013. 1

[4] E. Ilg, N. Mayer, T. Saikia, M. Keuper, A. Dosovitskiy, and T. Brox. Flownet 2.0: Evolution of optical flow estimation with deep networks. In *CVPR*, 2017. 1

[5] D. Krishnan, T. Tay, and R. Fergus. Blind deconvolution using a normalized sparsity measure. In *CVPR*, 2011. 18, 19, 20, 21, 22, 23, 24, 25, 26

[6] S. Nah, T. H. Kim, and K. M. Lee. Deep multi-scale convolutional neural network for dynamic scene deblurring. In *CVPR*, 2017. 1, 2, 3, 4, 5, 6, 7, 8, 9, 10, 11, 12, 13, 14, 15, 16, 17, 18, 19, 20, 21, 22, 23, 24, 25, 26

[7] J. Pan, Z. Hu, Z. Su, H.-Y. Lee, and M.-H. Yang. Soft-segmentation guided object motion deblurring. In *CVPR*, 2016. 1

[8] J. Pan, D. Sun, H. Pfister, and M.-H. Yang. Blind image deblurring using dark channel prior. In *CVPR*, 2016. 2, 3, 4, 5, 6, 7, 8, 9, 10, 11, 12, 13, 14, 15, 16, 17, 18, 19, 20, 21, 22, 23, 24, 25, 26

[9] S. Su, M. Delbracio, J. Wang, G. Sapiro, W. Heidrich, and O. Wang. Deep video deblurring. In *CVPR*, 2017. 1, 23, 24, 25, 26

[10] J. Sun, W. Cao, Z. Xu, and J. Ponce. Learning a convolutional neural network for non-uniform motion blur removal. In *CVPR*, 2015. 2, 3, 4, 5, 6, 7, 8, 9, 10, 11, 12, 13, 14, 15, 16, 17, 18, 19, 20, 21, 22, 23, 24, 25, 26

[11] O. Whyte, J. Sivic, A. Zisserman, and J. Ponce. Non-uniform deblurring for shaken images. *IJCV*, 2012. 2, 3, 4, 5, 6, 7, 8, 9, 10, 11, 12, 13, 14, 15, 16, 17, 18, 19, 20, 21, 22, 23, 24, 25, 26

[12] L. Xu, S. Zheng, and J. Jia. Unnatural l0 sparse representation for natural image deblurring. In *CVPR*, 2013. 2, 3, 4, 5, 6, 7, 8, 9, 10, 11, 12, 13, 14, 15, 16, 17, 18, 19, 20, 21, 22, 23, 24, 25, 26